

Chemical order and selection of the mechanism for strain relaxation in epitaxial FePd(Pt) thin layers

D. Halley,^{1,*} A. Marty,¹ P. Bayle-Guillemaud,¹ B. Gilles,² J. P. Attane,¹ and Y. Samson¹

¹CEA Grenoble/Département de Recherche Fondamentale sur la Matière Condensée, Service de Physique des Matériaux et Microstructures, 17 avenue des Martyrs, 38054 Grenoble Cedex, France

²Laboratoire de Thermodynamique et Physicochimie Métallurgiques/CNRS, BP 75, 38402 Saint Martin d'Hères, France

(Received 1 March 2004; revised manuscript received 1 June 2004; published 18 November 2004)

We observed that the relaxation mechanism of the epitaxial strain is dramatically dependent on the chemical ordering within the $L1_0$ structure in FePd(Pt) thin films. In disordered or weakly ordered layers, the relaxation takes place through perfect $\frac{1}{2}[101]$ dislocations, whereas well-ordered films relax through the partial $1/6[112]$ Shockley dislocations, piled-up within microtwins, with a huge impact on both the morphology and the magnetic properties of the film. We show that the antiphase boundary energy is the key factor preventing the propagation of perfect dislocations in ordered alloys.

DOI: 10.1103/PhysRevB.70.174438

PACS number(s): 61.72.Ff, 81.05.Bx, 81.40.Jj, 81.40.Rs

I. INTRODUCTION

Because of their extremely high technological importance, strain relaxation processes in thin epitaxial layers are widely studied. We focus here on the case of bidimensional growth, where strain relaxation occurs through the introduction of misfit dislocations. Such dislocations appear only above a given critical thickness, when the elastic energy accumulated within the layer is high enough to pay for their formation.¹ Depending on various parameters such as the crystalline structure of the layer,² the lattice mismatch with the substrate, the temperature of growth, the presence of threading dislocations in the substrate or in the buffer layer, the involved dislocations may be perfect or partial ones, isolated or piled up within extended defects.

In the specific case of chemically ordered alloys, the chemical order affects the energy cost associated with the propagation of the dislocations,² with a large effect on the plasticity and other mechanical properties. Here, we focus on thin films of chemically ordered magnetic alloys, such as FePd (FePt) grown on Pd (Pt) (001) substrates. Such alloys are seen as likely candidates for future high recording density magnetic media due to the large magnetocrystalline anisotropy associated with chemical ordering within the Au-Cu(I) type structure ($L1_0$) phase. We recently demonstrated that extended strain relaxation defects, namely, microtwins formed by the pileup of partial dislocations, are at the origin of a large magnetic coercivity, by providing pinning sites for the magnetic domain walls.³

The microtwins form through the pileup of $1/6[112]$ partial Shockley dislocations. The first partial dislocation glides from the surface of the film to the FePd/Pd (respectively, FePt/Pt) interface in order to make the film relax. Once one has appeared, the following ones preferably glide on adjacent $\{111\}$ planes so as to reduce the total stacking fault energy, thereby leading to the formation of the microtwins. We recently observed that the large repulsion between dislocation cores inside the microtwins controls the relaxation process and leads to an unusual dependence of the strain upon layer thickness, with a slow and almost linear relaxation curve. In

addition, a peculiar surface morphology is observed, with surface “steps” (up to 3 nm high) along the $\langle 110 \rangle$ directions. These steps correspond to the emergence of the microtwin at the layer surface and are easily observed by near field microscopies.⁴

However, we discovered that the microtwins are observed only when the growth process leads to a high degree of uniaxial chemical ordering within the $L1_0$ phase. Indeed, by playing with relevant parameters of the growth process, it is possible to grow chemically disordered thin layers of the same equiatomic FePd (FePt) alloys. Then, the relaxation takes place through the introduction of isolated perfect dislocations, thereby leading to dramatically different layer morphologies and magnetic properties. In this paper, we propose to describe, through experimental observations and modeling, the origin of the selection of a given relaxation process.

II. CHEMICAL ORDER, STRAIN, AND GROWTH PROCESS

Let us remind the reader that chemical ordering within the $L1_0$ phase corresponds to the formation of a stacking of chemically pure Fe and Pd (resp. Pt) (001) atomic planes defining two sublattices I and II. The perfectly ordered FePd alloy exhibits a quadratic structure ($a_c=0.372$ nm; $a_{a,b}=0.385$ nm) with c along $[001]$, leading to a lattice mismatch f ($f_{\text{ordered}}=1\%$) on the fcc Pd buffer layer ($a_{\text{Pd}}=0.389$ nm). The chemically disordered alloy has a fcc structure⁵ [$a_{\text{disordered}}=0.380$ nm), and an higher mismatch with respect to the Pd(001) substrate: $f_{\text{disordered}}=2.4\%$. For FePt on Pt buffer layer ($a_{\text{Pt}}=0.3916$ nm)], the corresponding data from Ref. 6 are ($a_{a,b \text{ ordered}}=0.386$ nm and $a_c=0.376$ nm, $f_{\text{ordered}}=1.5\%$). The lattice parameter for the disordered alloy is estimated according to $a_{\text{disordered}}=(a_c a_a^2)^{1/3}=0.3826$ nm and the mismatch $f_{\text{disordered}}=2.3\%$. The amount of chemical ordering of the equiatomic alloy is described by the long-range order parameter S where concentrations of Fe atoms on sites I or II are $C_{\text{I}}^{\text{Fe}}=(1+S)/2$ and $C_{\text{II}}^{\text{Fe}}=(1-S)/2$. Hence, S

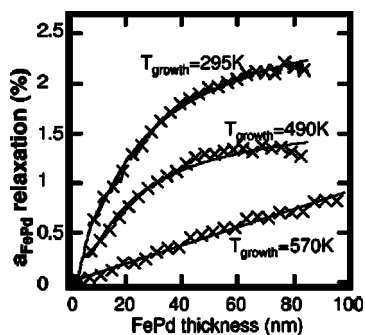


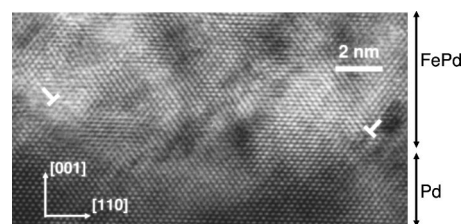
FIG. 1. FePd surface in-plane lattice parameter relaxation $[(a_{\text{FePd}(\text{surface})} - a_{\text{Pd}}) / a_{\text{Pd}}]$ measured during growth at various temperatures between 01 and $0\bar{1}$ rods on the RHEED diagram. A fit of the curves is given following Ref. 1 for growths at 295 and 490 K, and linear for the growth at 570 K.

ranges from 0 for a disordered alloy to 1 for a perfectly ordered alloy. S may be estimated from the ratio of integrated intensities of the superlattice (001) and (003) peaks to the fundamental (002) and (004) ones from x-ray diffraction measurements.⁷ Experimentally, well ordered alloys ($S = 0.8$) may be prepared through codeposition^{7,8} of both Fe and Pd (Pt) by molecular beam epitaxy at an high enough temperature (600–750 K) on Pd (Pt) (001) substrates, while a chemically disordered film is obtained for growth at room temperature. Partial chemical order may be obtained at intermediate growth temperatures. A detailed description of the growth process has been provided previously.^{7,9}

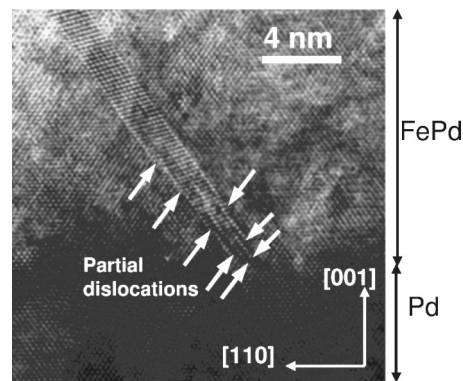
In the following, to be able to separate the effect of the growth temperature from other parameters, we also rely on a specific growth process, where the $L1_0$ stacking is artificially obtained by alternated deposition of pure Fe and Pd (or Pt) monoatomic planes. Such films, grown at room temperature, exhibit a negligible (FePd, $S \sim 0.1$) or significant (FePt, $S \sim 0.5$) long-range order.¹⁰ It is likely that this difference is associated with the higher surface mobility of the Pd atoms (with respect to Pt) that leads to more layer mixing during the layer by layer growth process, and finally to a lower chemical order.

III. RESULTS

We determined the evolution of the in-plane lattice parameter during the codeposition of FePd on Pd substrate by measuring the distance between 01 and $0\bar{1}$ rods on the Reflection high energy electron diffraction (RHEED) pattern (Fig. 1). Three growth temperatures were used, leading to different long-range order parameters as determined *ex situ* by x-ray diffraction: $T_{\text{growth}} = 295$ K ($S = 0$); $T_{\text{growth}} = 490$ K ($S = 0.15$); and $T_{\text{growth}} = 570$ K, ($S = 0.8$). As the unstrained lattice parameter of the alloy depends on the amount of chemical ordering, we observe these different lattice mismatches on RHEED curves. For thick FePd films (thicker than 80 nm), the complete relaxation is close to 2.4% in disordered films and to 0.9% in well-ordered films. Partially ordered layers have relaxed of 1.4%; this value is in between the values reached for ordered and disordered layers.



(a)



(b)

FIG. 2. HRTEM images of $[110]$ cross-sections on FePd samples (a) $T_{\text{growth}} = 470$ K: we just observe $\frac{1}{2}\langle 110 \rangle$ perfect dislocation lines; (b) $T_{\text{growth}} = 620$ K microtwins appear parallel to $\{111\}$ planes, and we also observe a few perfect dislocations.

The approximately linear shape of the relaxation curve of the ordered layer grown at 573 K can be ascribed to the repulsion between dislocation cores inside microtwins. As detailed elsewhere,⁴ once a microtwin is formed, the pileup of a new dislocation within the same defect is allowed only when the thickness has increased enough so as to provide a new stable position for an additional dislocation. Modeling demonstrated that this leads indeed to a relaxation constant rate. Conversely, in the case of growth at 300 and 473 K, we do not observe such linear relaxation curves, but ones exhibiting more common shapes that could be fitted with a model derived from the well-known Matthews equation.^{1,11} This suggests the absence of microtwinning within these films. In order to check this last assumption, we observed the surface³ of the different samples by *ex situ* AFM (atomic force microscopy). Indeed, the intersection of the microtwins with the (001) plane corresponding to the free surface of the thin layer leads to the appearance of easily detectable steps along $\langle 110 \rangle$ directions.⁴ On the two samples grown at 300 K (disordered one) and 470 K (partially ordered one), we do not observe such straight steps. The strain relaxation process active here has been determined by high-resolution transmission electron microscopy (HRTEM). In section images [Fig. 2(a)] obtained on weakly ordered layers, we do not observe microtwins but $\frac{1}{2}[101]$ perfect dislocations within the FePd layer, close to the FePd/Pd interface. These dislocations exhibiting an in-plane component of the Burgers vector contribute to the strain relaxation. So, as suggested by RHEED and AFM measurements, the relaxation takes place by microtwinning only in well chemically ordered films [Fig. 2(b)], whereas the perfect dislocations are the only strain

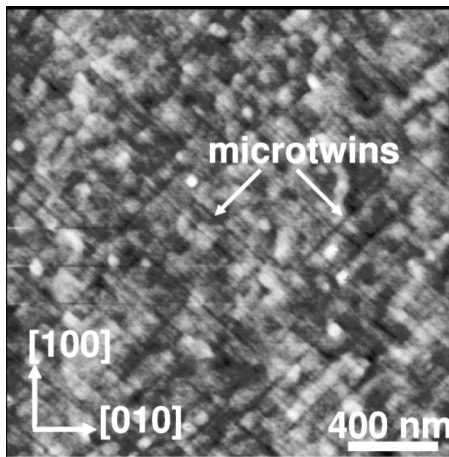


FIG. 3. *Ex situ* AFM image obtained on a 40 nm FePt films capped with 1.5 nm Pt: layer-by-layer growth at $T_{\text{growth}}=300$ K ($S=0.45$). Microtwins appear on the surface as long lines along $\langle 110 \rangle$.

relaxation defects in chemically disordered films.

The same link between chemical order and the strain relaxation process is observed in FePt/Pt films: microtwins are observed³ by AFM in films grown at 750 K that are chemically well ordered ($S=0.8$) whereas the images do not show any microtwin in disordered alloy co-deposited at 300 K.

As we relied on the growth temperature to induce different states of chemical orders, the occurrence of two relaxation mechanisms could be attributed to the effect of different temperatures on dislocations mobility and/or nucleation. However, we can rule out the role of temperature in FePt as well-ordered thin films can be grown at room temperature. Indeed, chemically ordered FePt thin films are obtained at room temperature by atomic layer by atomic layer growth ($S=0.5$): Microtwins are then observed on AFM images (Fig. 3). FePd films grown by a similar layer-by-layer at 300 K exhibit a low chemical order ($S=0.1$). Consistently, these films do not exhibit microtwins.

Moreover, the different misfit f in the case of ordered and disordered alloys seems not to be the cause of the different relaxation mechanisms: Ordered FePd layers grown on a Pt buffer with a higher misfit ($f=1.5\%$) also exhibit microtwins (not shown here).

$1/2[101]$ perfect dislocations do not have to nucleate in the FePd and FePt layers as there are already such numerous threading dislocations due to the relaxation of the Pd buffer on the MgO substrate. A high density of these dislocations was observed by HRTEM. Moreover, on scanning tunneling microscopy images of the Pd buffer layer⁸ these dislocations were observed as screws at the Pd surface (up to 10^3 screws/ μm^2). Nucleation barriers might thus not limit the relaxation of the film via $1/2[101]$ perfect dislocations, as they just have to propagate and not to nucleate. Concerning partial dislocations, they may appear by nucleation or by dissociation of the perfect one's in their $(1\bar{1}1)$ gliding plane, i.e., a threading perfect dislocation $1/2[101]$ may be decomposed in two partial dislocations, $1/6[112]$ and $1/6[2\bar{1}1]$. The first one being pure edge at the interface will be efficient for the relaxation process. This suggests that, within chemi-

cally ordered thin films, the relaxation by partial Shockley dislocations has to be linked with a lower slip energy cost for these dislocations compared to perfect dislocations.

IV. CHEMICAL ORDER AND ENERGY COST OF DISLOCATIONS

Here we first explain how chemical ordering can have a large influence on the energy cost of dislocations. We will next propose a quantitative estimation of the effect.

In the case of a $L1_0$ ordered structure with the quadratic c axis along $[001]$, the propagation of a $1/2[101]$ perfect dislocation creates an antiphase boundary (APB) along the $\{111\}$ gliding plane within the ordered structure.² Indeed, on both sides of the glide plane of such a dislocation, pure Fe and Pd(Pt) planes are out of phase. We have to take into account an extra APB energy for the propagation of these perfect dislocations in the case of well-ordered films. A rough evaluation of this APB energy can be done in the following way: We attribute a bounding energy J to Fe—Fe or Pd—Pd homocoordination and $-J$ to heterocoordination Fe—Pd nearest neighbor pairs. An estimate of J may be obtained from the order-disorder transition temperature T_c within the Ising model:¹² $K_B T_c \sim 1.74J$.

Since T_c is close to 900 K for the equiatomic alloy, we find a rough approximation for $J: J \approx 4.5 \times 10^{-2}$ eV. As the creation of an APB along a $\{111\}$ plane breaks one Fe—Pd heterocoordination bond (there are seven heterocoordination bonds on such an APB compared to eight in a perfectly ordered structure), we can evaluate the APB energy cost at $2J$ per atom of the APB. The atoms density being $4/(a^2 \times \sqrt{3})$ on $\{111\}$ planes, the APB energy formed by $1/2[101]$ dislocations may be written as: $\gamma_{111}^{\text{APB}} = 4/(a^2 \times \sqrt{3})2J \approx 0.2$ J/m².

This assessment is made under the hypothesis that the APB crosses a perfectly $L1_0$ ordered structure. In fact, the short-range order might be incomplete, [for instance for layer-by-layer grown films where the long-range order parameter is lower than 0.5]. So, the obtained value (0.2 J/m²) might be seen as the maximum one reached by $\gamma_{111}^{\text{APB}}$.

Concerning $1/6[112]$ partial dislocations, the total stacking fault energy $\gamma_{111}^{\text{partial}}$ should take into account the modification of both the positions of the atoms and of their chemical environment along the gliding plane. These are commonly² seen as the sum of two independent terms: $\gamma_{111}^{\text{partial}} = \gamma_{111}^{\text{stacking}} + \gamma_{111}^{\text{chemical}}$. For the structural part $\gamma_{111}^{\text{stacking}}$, we take an average of the stacking fault energy^{13,14} in fcc Pd and Fe. This yields $\gamma_{111}^{\text{stacking}} \approx 0.16$ J/m². Then, the chemical part of the total stacking fault turns out to be negligible: A careful study of the partial dislocation glide plane shows that the number of Fe—Pd bounds remains unchanged ($N_{\text{Fe—Pd}}=8$) in the case of a $1/6[112]$ dislocation within a chemically ordered structure, with the c axis along $[001]$. As a result, we neglect $\gamma_{111}^{\text{chemical}}$, and $\gamma_{111}^{\text{partial}} \approx 0.16$ J/m², approximately independent from the chemical order.

Next, we can compare the forces exerted on perfect and partial dislocations in ordered and disordered FePd alloys. We consider a dislocation lying at the FePd/Pd interface

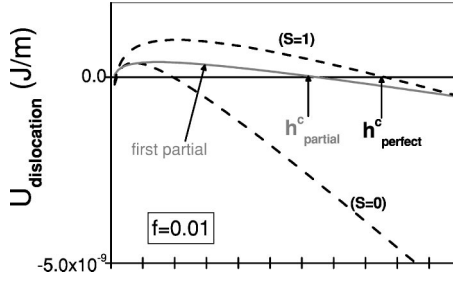


FIG. 4. Energy per unit length for dislocations buried at the FePd/Pd interface, supposing a tensile lattice strain $f=0.01$ in FePd: (line) isolated $1/6[112]$ partial dislocations (first partial); (dots) $1/2[101]$ perfect dislocations, neglecting the APB energy (i.e., supposing $S=0$) or taking the APB energy into account (supposing $S=1$). The critical thicknesses for strain relaxation h_c are indicated for both types of dislocations in the case of a perfectly FePd ordered alloy ($S=1$): $h_c=12$ nm for partial dislocations and $h_c=17$ nm for perfect dislocations.

with a threading arm crossing the film up to the surface. The force exerted on this threading arm (supposed to remain parallel to itself) corresponds to the energy to propagate the dislocation of a unit length. The total energy of the dislocation per length unit U_{tot} is the sum of the self-energy density U_{self} ,¹⁵ of the interaction energy of the dislocation with the stressed film U_{int} , and of the energy of the faulted area U_{fault} created along the glide plane.

These energy densities can be written

$$U_{\text{self}} = \frac{\mu b^2 (1 - \nu \cos^2 \beta)}{4\pi(1 - \nu)} \ln\left(\frac{\alpha h}{b}\right),$$

$$U_{\text{int}} = -2\mu \frac{1 + \nu}{1 - \nu} f h b \times \sin(\beta) \cos(\phi),$$

$$U_{\text{fault}} = h \gamma_{111} / \sin(\phi),$$

where h is the depth of the dislocation beneath the free surface, ν the Poisson's ratio, μ the shear modulus, b the modulus of the Burgers vector. The glide system is defined by the angle β between the Burgers vector and the dislocation line and ϕ is the angle between the glide plane and the surface of the epilayer. α is the core parameter; it is linked to these constants and to the core energy of the dislocation.¹⁶ α can be taken equal to 1 for both perfect and partial dislocations, varying α between the 0.6 and 4 extreme possible values leading to negligible changes in the energy curves. f is the misfit between the buffer layer and the epilayer. For the tilted $\{111\}$ glide plane $\phi=54.7^\circ$, $\beta=90^\circ$ for the partials dislocation and $\beta=60^\circ$ for perfect dislocations. γ_{111} is the fault energy density, i.e., $\gamma_{111}^{\text{partial}}$ for partials dislocation or $\gamma_{111}^{\text{APB}}$ for perfect ones.

We calculated $U_{\text{tot}}(h)$ as a function of the FePd thickness for the next cases (Fig. 4):

- Perfect dislocations embedded in disordered alloy ($S=0$) i.e., without APB energy.
- Perfect dislocations embedded in ordered alloy ($S=1$) with APB energy.

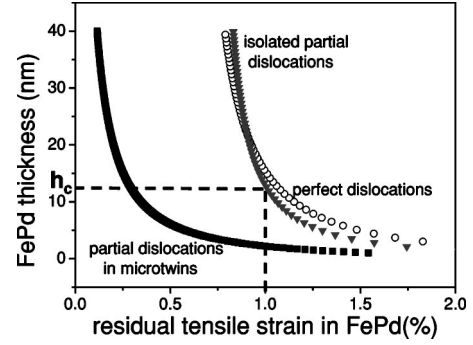


FIG. 5. Calculated critical thickness for the propagation of isolated $1/6[112]$ partial dislocations and $1/2[101]$ perfect dislocations as a function of the tensile strain in a perfectly ordered FePd layer ($S=1$). We took into account the APB and stacking fault energy associated with both kinds of dislocations. The critical thickness is smaller for partial dislocations than for perfect ones for $f > 0.9\%$ (we find again $h_c=12$ nm for 1% initial tensile strain). The critical thickness for partial dislocations in microtwins (without stacking fault energy) is much below the values obtained for isolated dislocations.

- Partial dislocations with stacking fault energy.

The critical thickness for the propagation of a type of dislocation occurs when $U_{\text{tot}}(h_c) = 0$.

The influence of the extra energy due to APB is striking: In ordered films, the critical thickness for $1/6[112]$ partial dislocations ($h_c \sim 12$ nm) is lower than for $1/2[101]$ perfect dislocations ($h_c \sim 17$ nm) but, in disordered films, h_c ($1/2[101]$) falls to 4 nm, reversing the preferred strain relaxation defect. Hence, the propagation of partial dislocations is favored at the beginning of the growth within chemically ordered layers.

The critical thickness h_c for dislocations propagation can be systematically calculated as a function of the tensile strain f : It gives $h_c = [b(1 - \nu \times \cos^2 \beta)] / [8\pi(1 + \nu) \times (f - f_c) \sin \beta \cos \phi \ln(\alpha h_c / b)]$, with $f_c = (1 - \nu) / (1 + \nu) \times (\mu b \sin \beta \cos \phi)$ and $\gamma = \gamma^{\text{partial}}$ or γ^{APB} . Figure 5 shows this critical thickness in a perfectly ordered FePd layer for both types of dislocations. It clearly shows that for $f > 0.9\%$, partial dislocations propagate before perfect dislocations. That is the case for well-ordered alloys in which $f=1\%$.

This applies for the very first (isolated) partial dislocations. Once the first ones have nucleated and propagated, the relaxation might continue by the nucleation of new partials close to the former ones. This differs from the case we considered in Fig. 4, our calculation providing the energy cost of a lonely dislocation. Actually, the following partial dislocations glide along the preexisting gliding plane,⁴ thus sparing the $\gamma_{111}^{\text{stacking}}$ stacking fault energy. The stacking fault energy is as usual² assumed to be equal to twice the twinning fault energy. Hence, whatever the number of partial dislocations piled up within the microtwin, the fault energy associated with the microtwin does not increase. This clearly reduces the energy cost of these new partial dislocations (Fig. 5), and explains why, the microtwins being formed, adding new partial dislocation to the preexisting defects (rather than forming perfect ones) is the favored process even for thick layers of alloy.

V. CONCLUSION

The influence of the chemical ordering on the selection of the mechanism for the relaxation of the epitaxial strain in FePd alloys proved to be determinant: The epitaxial strain is relaxed via microtwins within chemically ordered films and in chemically disordered ones via the introduction of perfect $1/2[101]$ dislocations at the buffer/layer interface. Indeed, $1/2[101]$ dislocations introduce an extra chemical stacking fault energy within the chemically ordered $L1_0$ structure, thereby favoring partial dislocations in well-ordered layers. As partial dislocations piled up within extended defects, this leads to the formation of microtwins with dramatic consequences on the morphology of the thin layer. This may be the instance of such an effect within metallic systems.

Two comments seems now worthy of interest. First, it has been recently demonstrated that these structural defects provide pinning sites for the magnetic domain walls within FePt thin films, and are then at the origin of an exceptionally large coercitive field.³ As chemically ordered alloys may be used within the next generations of high recording density magnetic media, the link we demonstrate here between structural defects and chemical order should be taken into account. Next, within the description we propose, the extra-stacking fault for $1/2 [101]$ dislocations depends primarily on the short-range chemical order. As the magnetocrystalline anisotropy depends on the same parameter,¹⁷ it may not be possible to adjust this anisotropy independently of the structural defects occurring within thin layers of chemically ordered alloys.

*Corresponding author. Electronic mail: halley@drfmc.ceng.cea.fr

¹J. W. Matthews and A. E. Blakeslee, *J. Cryst. Growth* **27**, 118, (1974).

²J. P. Hirth and J. Lothe, *Theory of Dislocations*, 2nd ed. (Wiley & Sons, New York, 1982).

³J. P. Attané, Y. Samson, A. Marty, D. Halley, and C. Beigné, *Appl. Phys. Lett.* **79**, 794 (2001).

⁴D. Halley, Y. Samson, A. Marty, P. Bayle-Guillemaud, C. Beigné, B. Gilles, and J. E. Mazille, *Phys. Rev. B* **65**, 205408 (2002).

⁵W. B. Pearson, *Handbook of Lattice Spacings and Structures of Metals* (Pergamon, New York, 1964).

⁶E. A. Brandes and G. B. Brook, *Smithells Metals Reference Book*, 7th ed. (Butterworths-Einemann, Oxford, 1997).

⁷V. Gehanno, A. Marty, B. Gilles, and Y. Samson, *Phys. Rev. B* **55**, 12552 (1997).

⁸B. Gilles, F. F. Xu, D. Halley, A. Marty, Y. Samson, and G. Patrat, *Mater. Res. Soc. Symp. Proc.* **614**, 1 (2001).

⁹D. Halley, Y. Samson, A. Marty, C. Beigne, and B. Gilles, *Surf.*

Sci. **481**, 25, (2001).

¹⁰K. Sato, E. Takeda, M. Akita, M. Yamaguchi, K. Takanashi, S. Mitahi, H. Fujimori, and Y. Suzuki, *J. Appl. Phys.* **86**, 4985 (1999).

¹¹G. Bochi, C. A. Ballentine, H. E. Inglefield, C. V. Thompson, R. C. O. Handley, J. H. Hug, B. Stiefel, A. Moser, and H. J. Guntherodt, *Phys. Rev. B* **52**, 7311 (1995).

¹²D. F. Styer, *Phys. Rev. B* **32**, 393 (1985).

¹³I. L. Dilamore and R. E. Smallman, *Philos. Mag.* **12**, 191 (1965).

¹⁴P. N. Okrainets and V. K. Pishak, *Metallofiz. Noveishie Tekhnol.* **72**, 31 (1978).

¹⁵M. Dynna, T. Okada, and G. C. Weatherly, *Acta Metall. Mater.* **42**, 1661, (1994).

¹⁶M. Dynna, A. Marty, B. Gilles, and G. Patrat, *Acta Mater.* **44**, 4417 (1996).

¹⁷V. Gehanno, C. Revenant-Brizard, A. Marty, and B. Gilles, *J. Appl. Phys.* **84**, 2316 (1998).